Planar Detectors as Radiometric Standards using Carbon Nanotube Absorbers

Malcolm White

National Institute of Standards and Technology
325 Broadway, Boulder, CO 80305-3228
m.white@boulder.nist.gov

Calcon 2017
Logan, Utah

Radiometry R&D:
John Lehman
Michelle Stephens
Ivan Ryger
Thomas Gerrits
Nathan Tomlin
Malcolm White
Chris Yung
Igor Vayshenker
Zeus Ruiz Gutierrez

www.calcon.sdl.usu.edu

PHYSICAL MEASUREMENT LABORATORY

National Institute of Standards and Technology
U.S. Department of Commerce

Outline

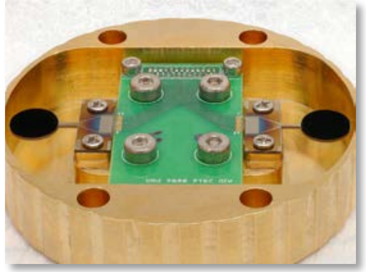

Chip Design

Integration

Results

Motivation – new radiant power standards

- open beam
- 850 nm
- 1310, 1550 nm

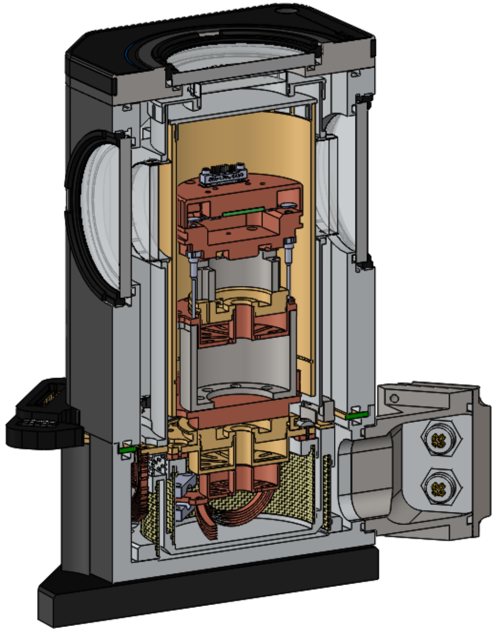

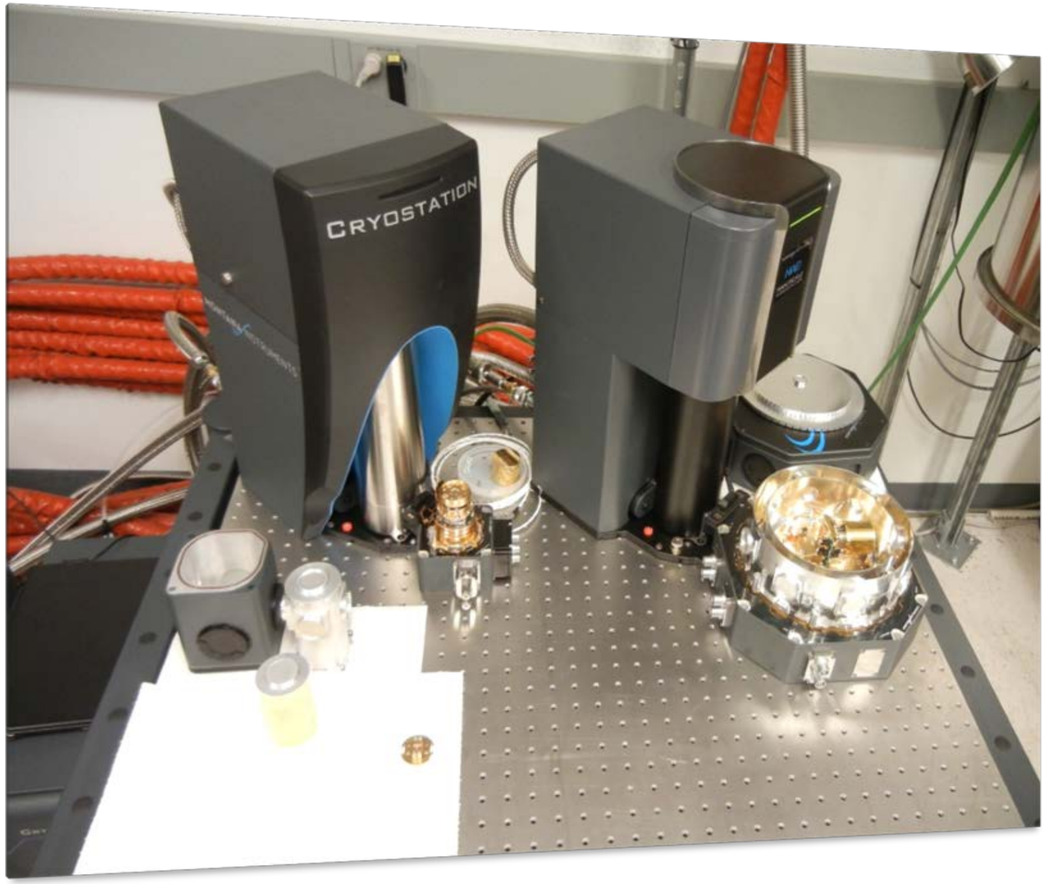

Carbon nanotube detector

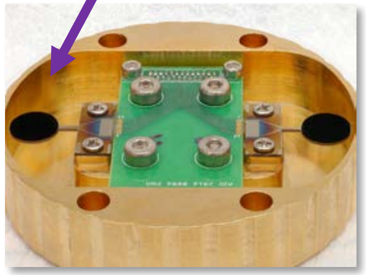

Chip Design – close up of patterning

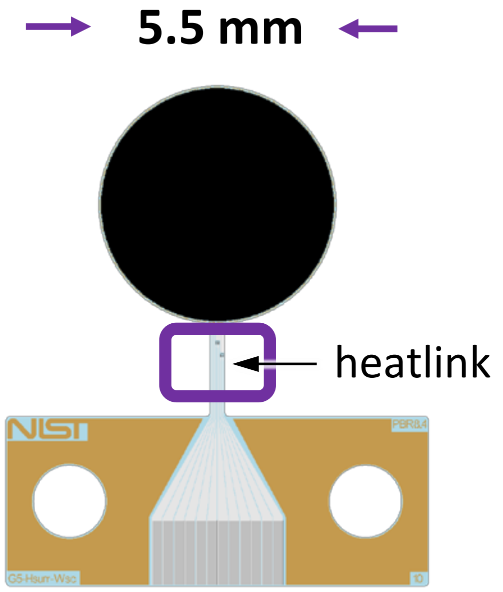

2.0 x 0.375 x 0.4 mm wide

Position of Nb TESs and Vanadium superconducting leads

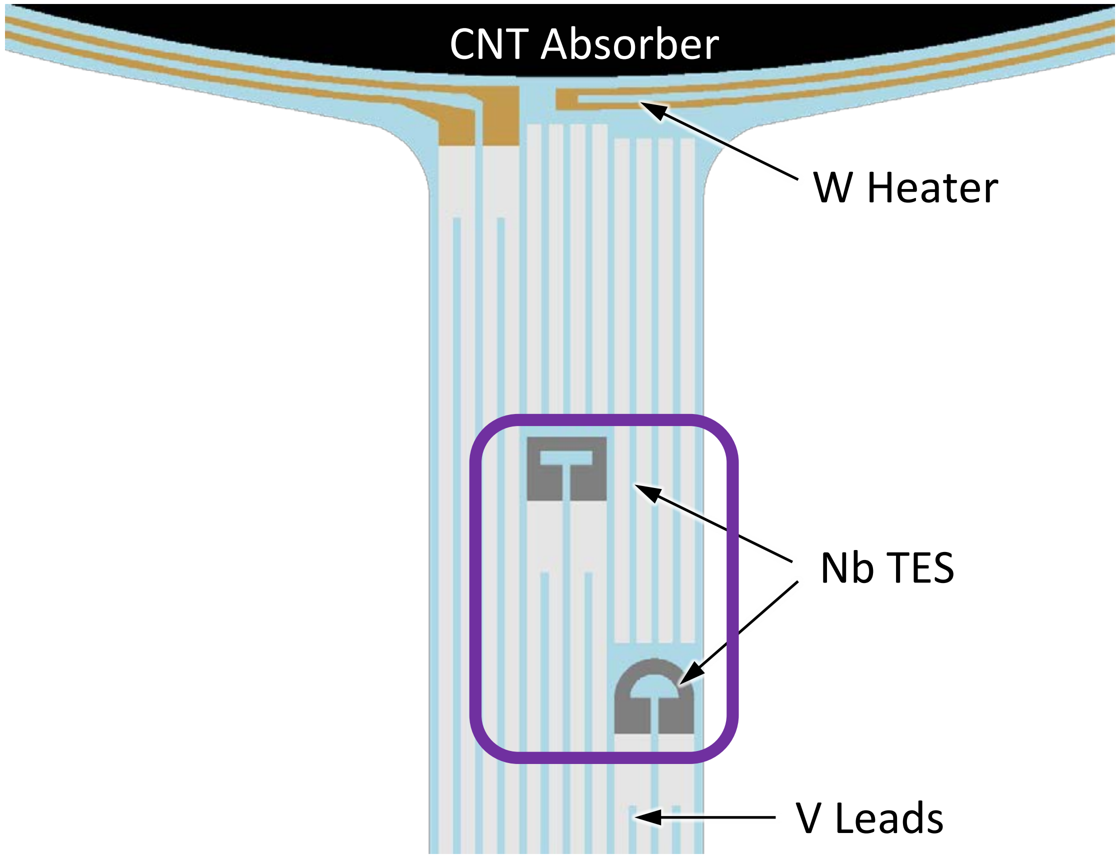

Chip Design – side view of lithographic pattern

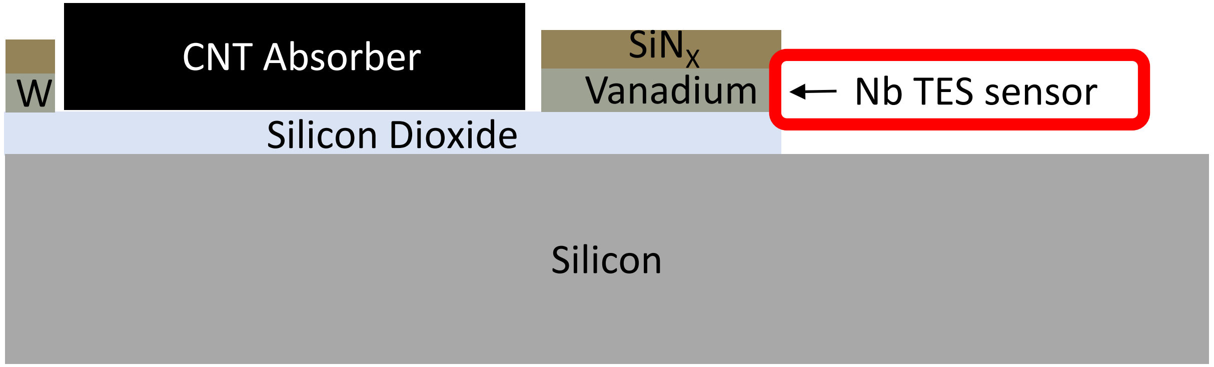

Layers:

- Silicon substrate: 375 µm
- SiO_2 insulator: 150 nm
- W heater: 44 nm
- Nb TES sensor: 93 nm
- V wiring: 146 nm
- SiN_x passivation layer: 170 nm
- Catalyst: 10 nm Al_2O_3 + 1 nm Fe
- Si deep etch
- VACNT growth: 400 µm

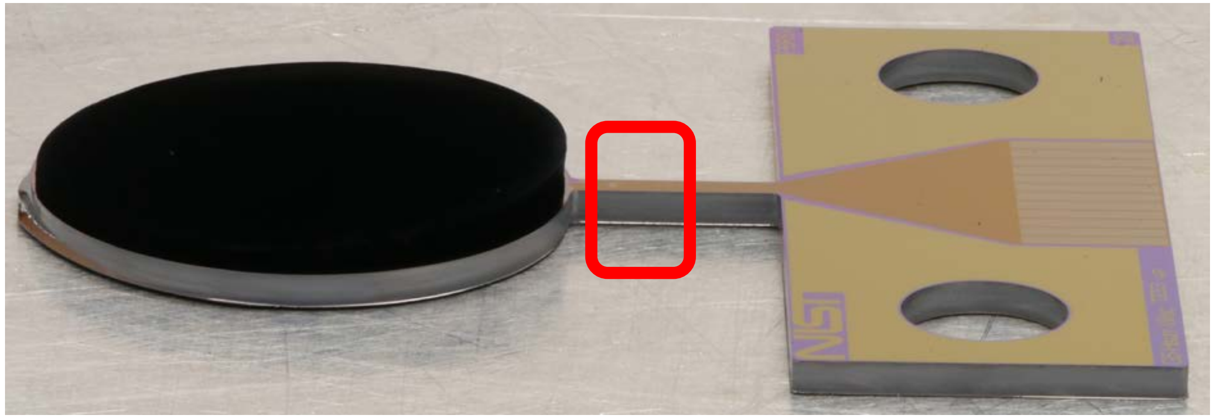

Chip Design – nanotube growth

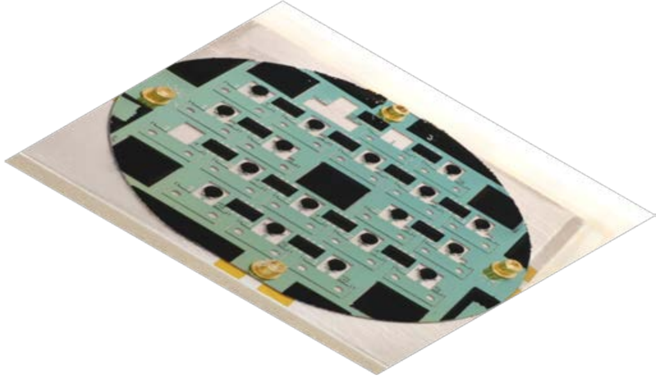

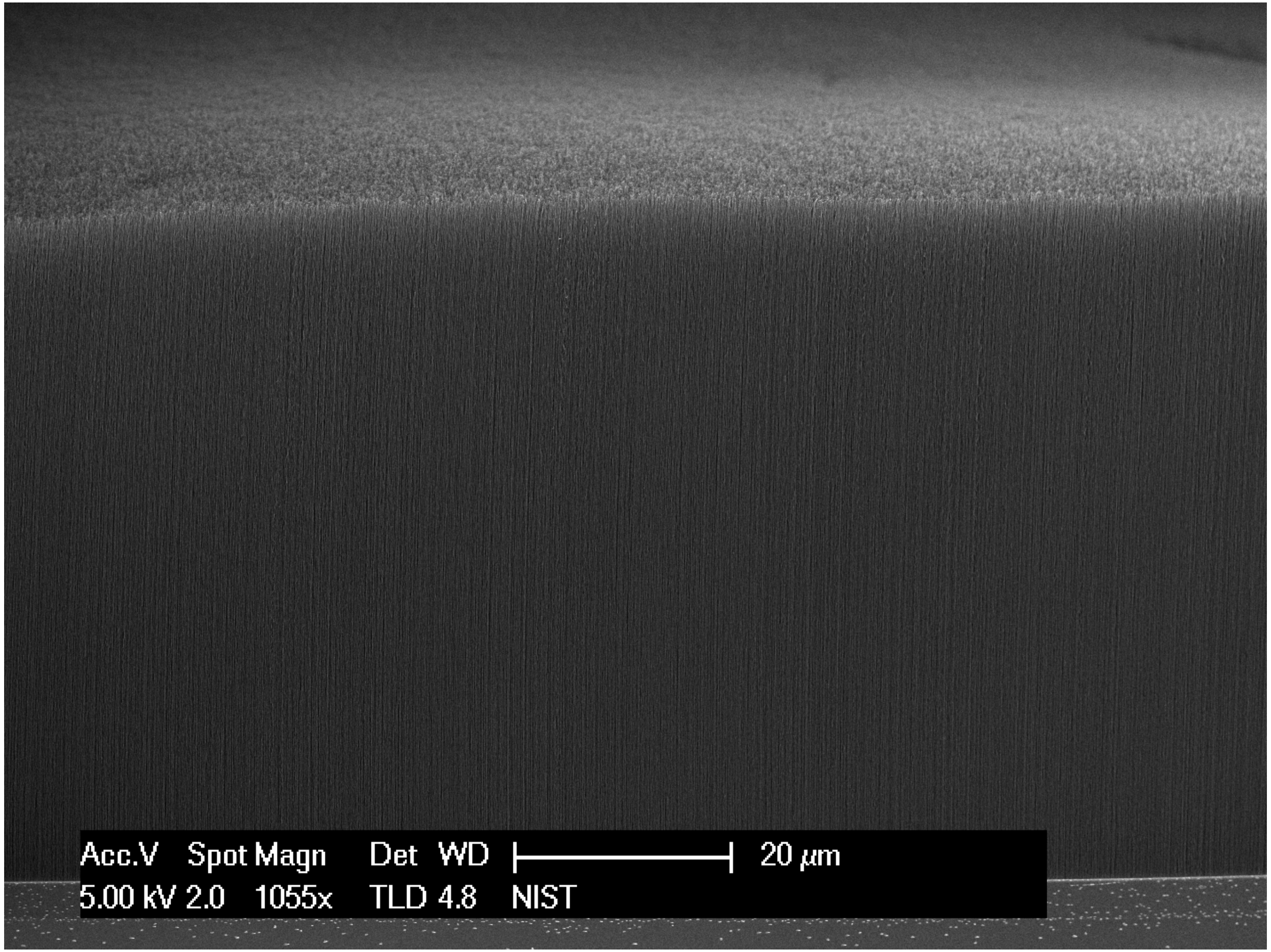

Chip Design – post growth processes

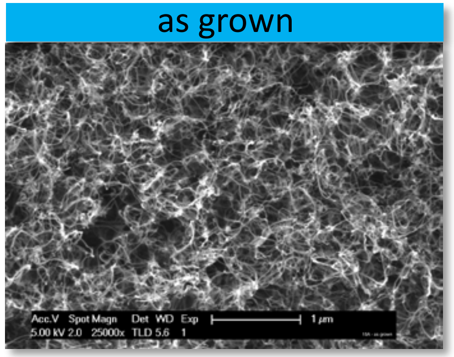

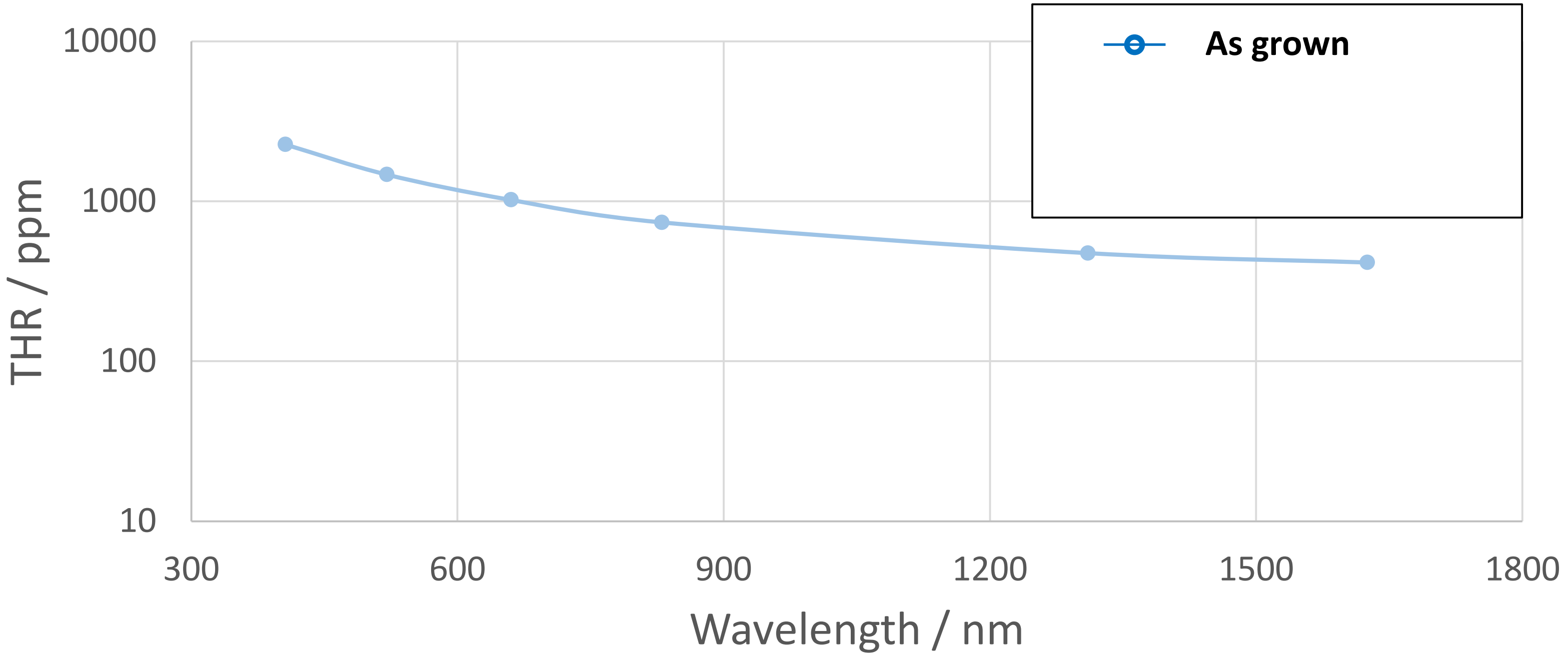

Chip Design – post growth processes

as grown

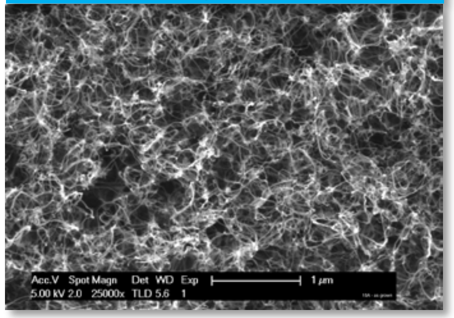

200 W @ 60 s

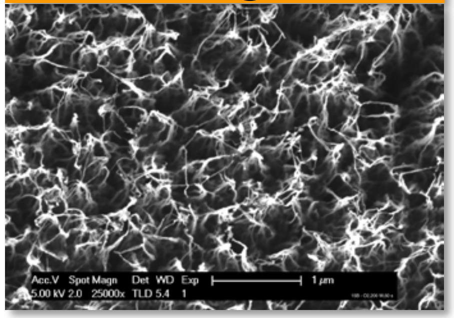

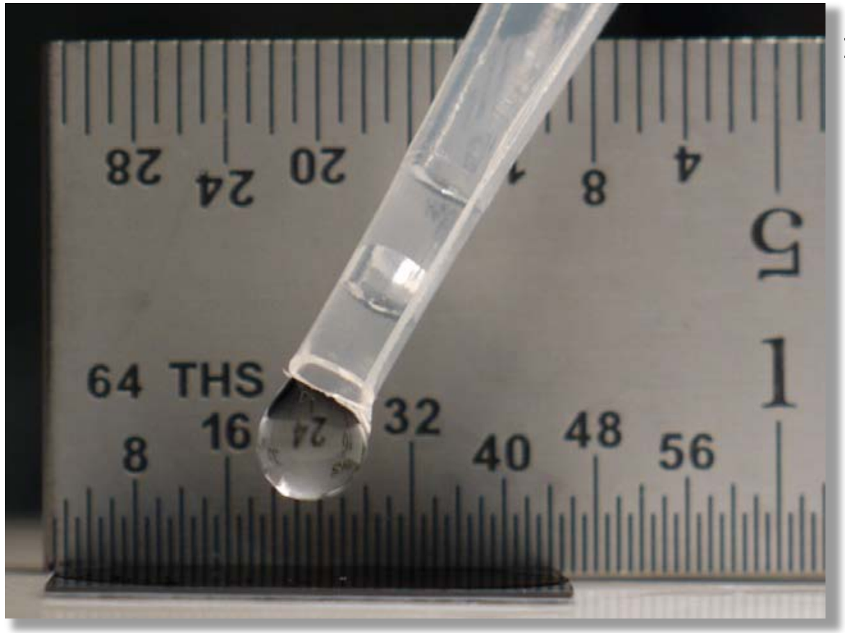

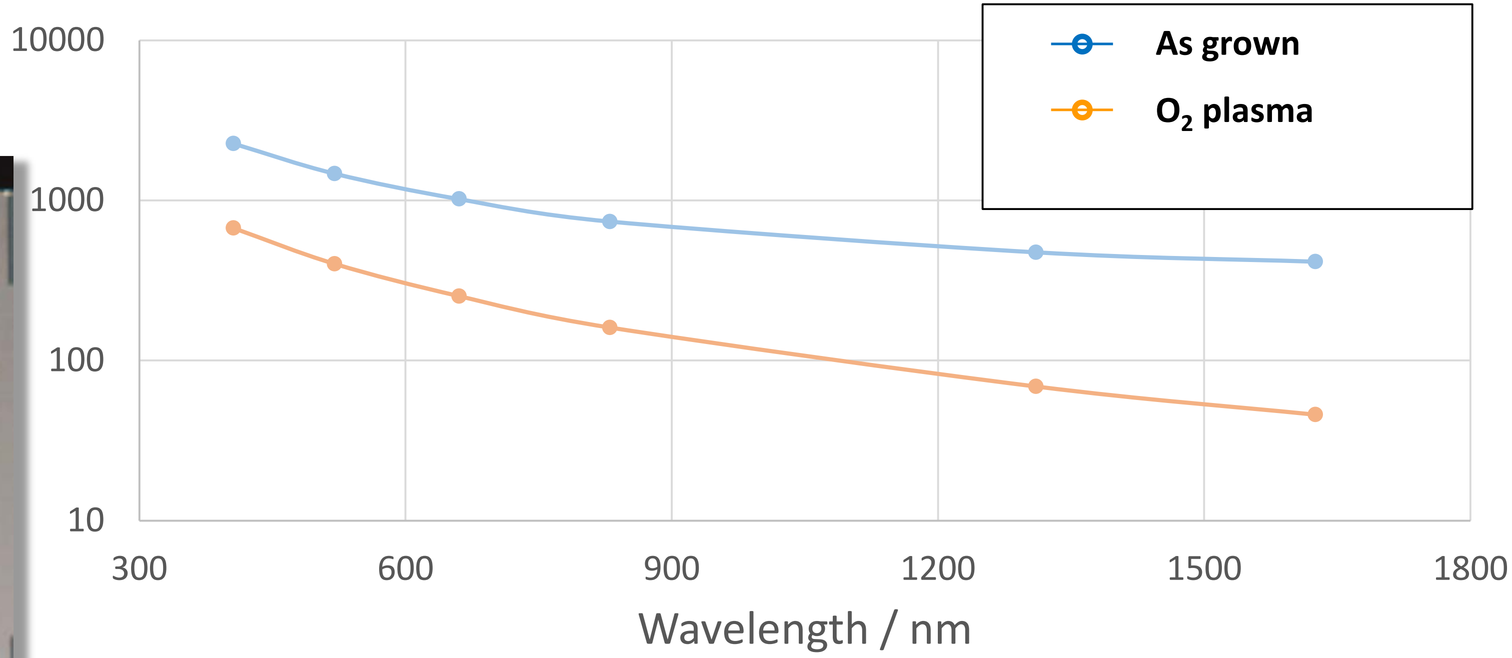

Chip Design – post growth processes

as grown

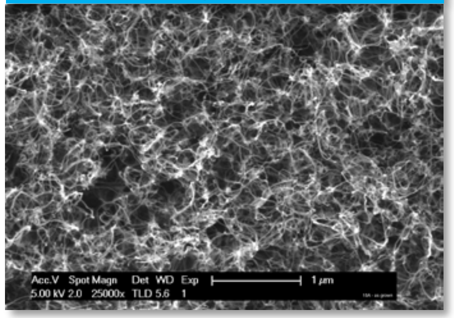

200 W @ 60 s

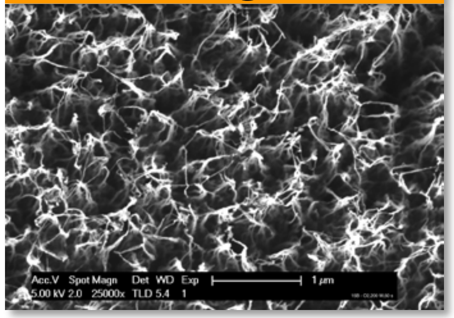

30 W @ 40 s

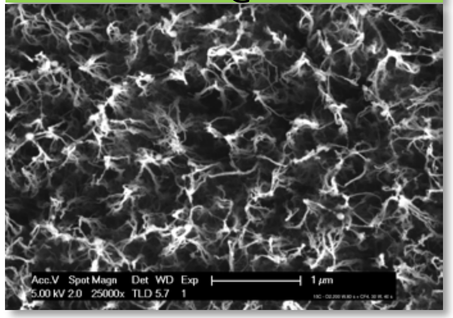

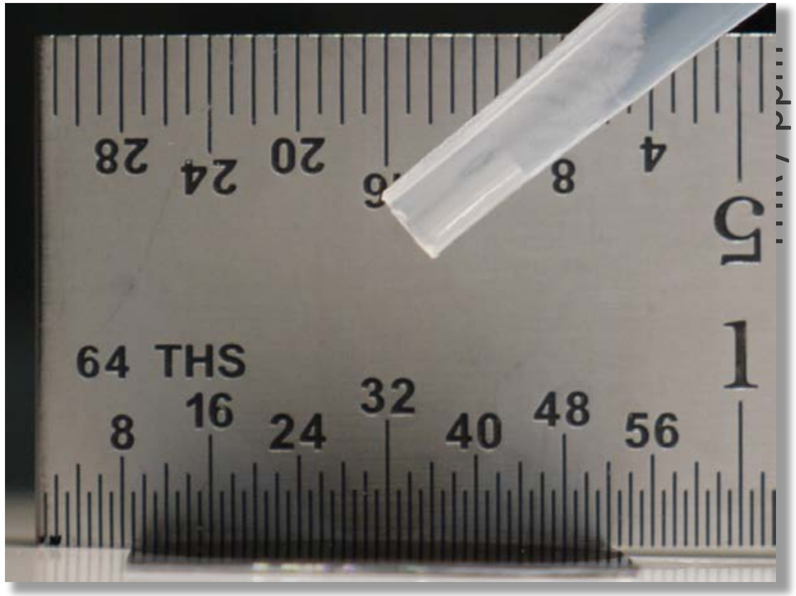

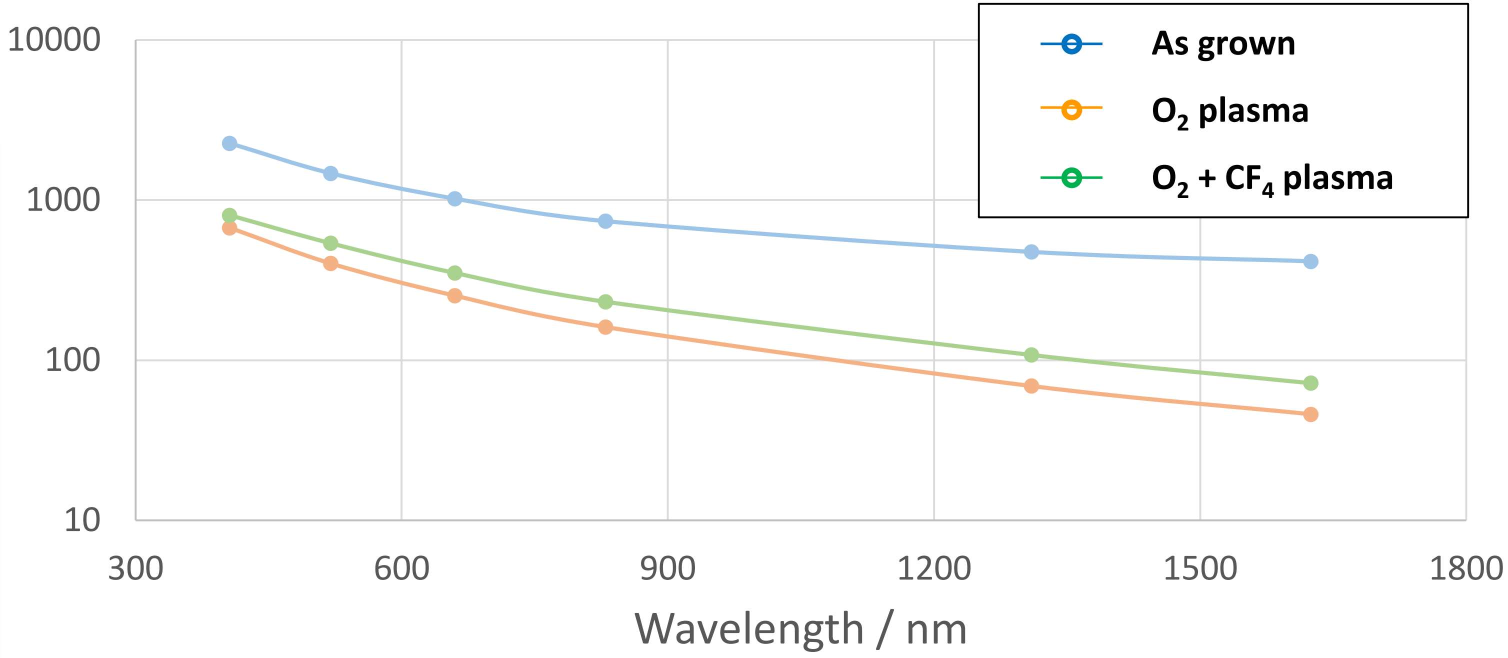

Chip design – absolute reflectance LASP

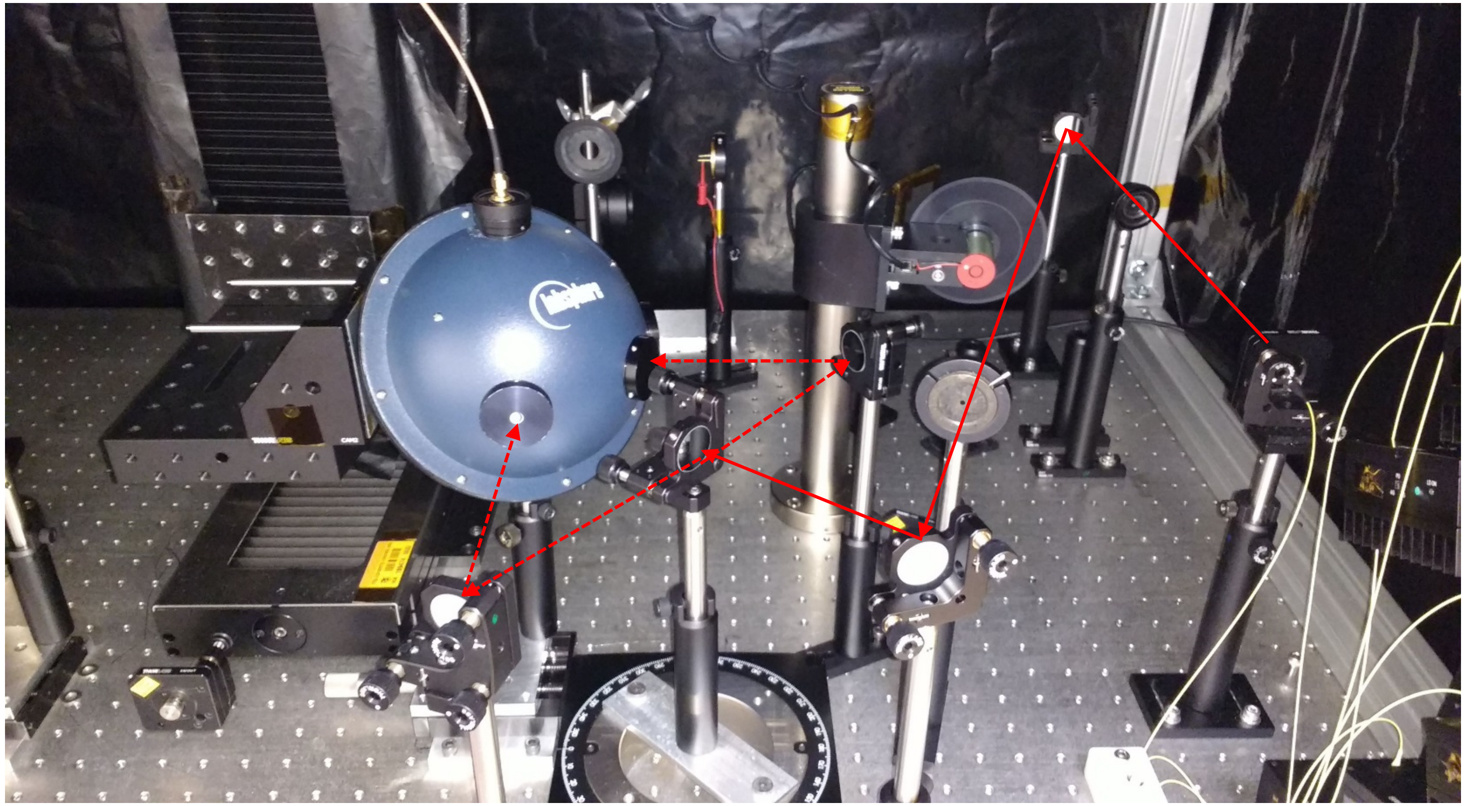

Credit: Karl Heuerman, LASP

Laser based reflectometer - measure absolute total hemispherical reflectance from 406 nm to 1625 nm and 10.6 µm

Can raster scan the sample

Chip design – absolute reflectance scan @ 1310 nm

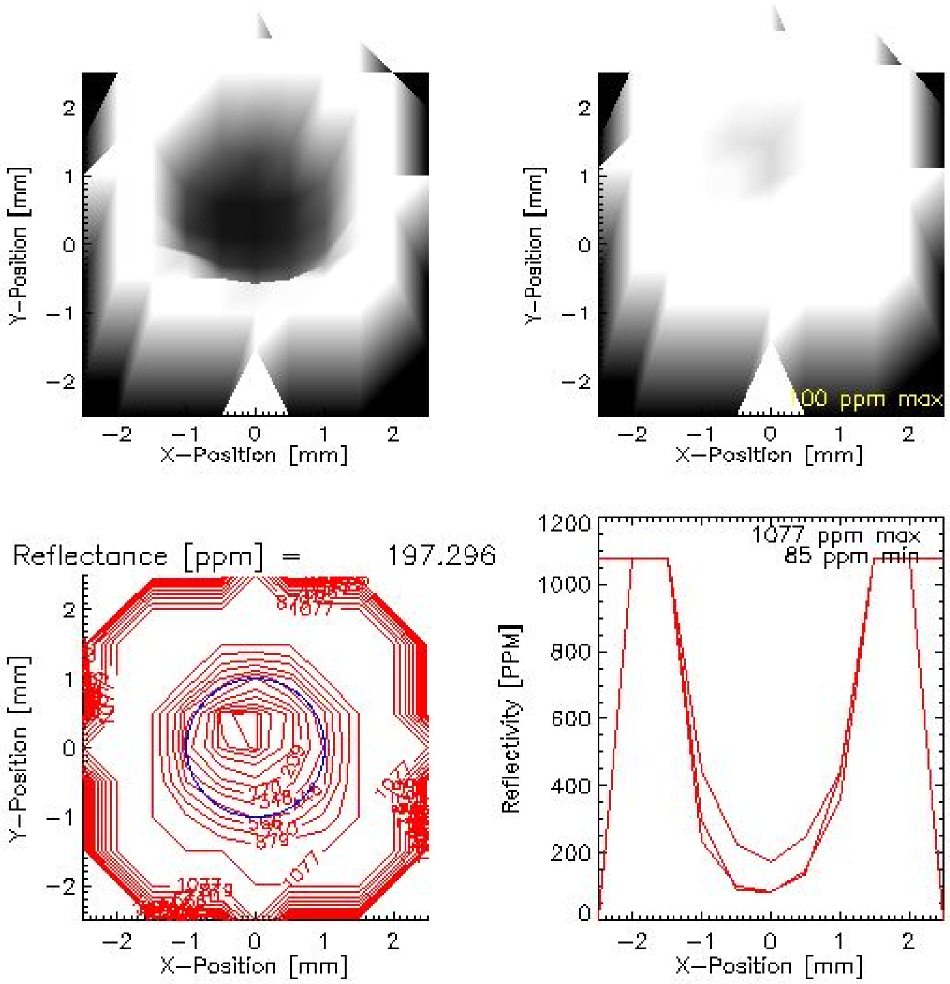

830 nm 102 ppm
1310 nm 197 ppm
1625 nm 304 ppm

O_2, 200 W, 60 s, don't break vacuum CF_4, 30 W, 40 s

Chip design – sensor & superconducting wiring

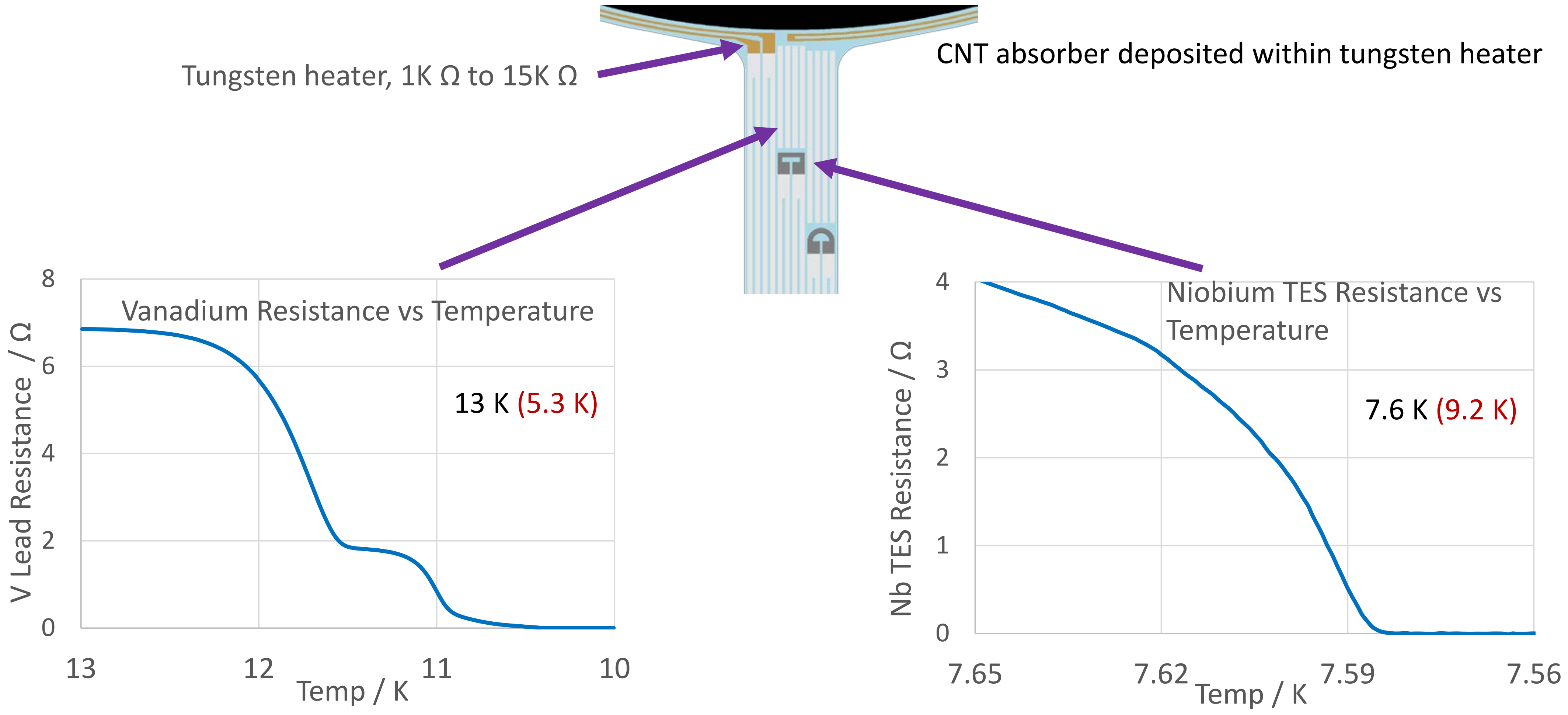

N.A. Tomlin, M. White, I. Vayshenker, S.I. Woods, J.H. Lehman, Metrologia ***52****, 2, 376 – 383 (2015). http://dx.doi.org/10.1088/0026-1394/52/2/376*

Integration – fibre radiometer (ESR)

- Operation at 300 µW
  - 850 nm
  - 1310, 1550 nm

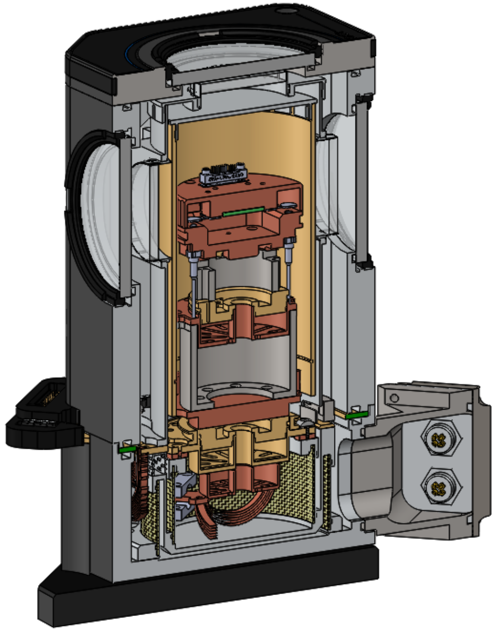

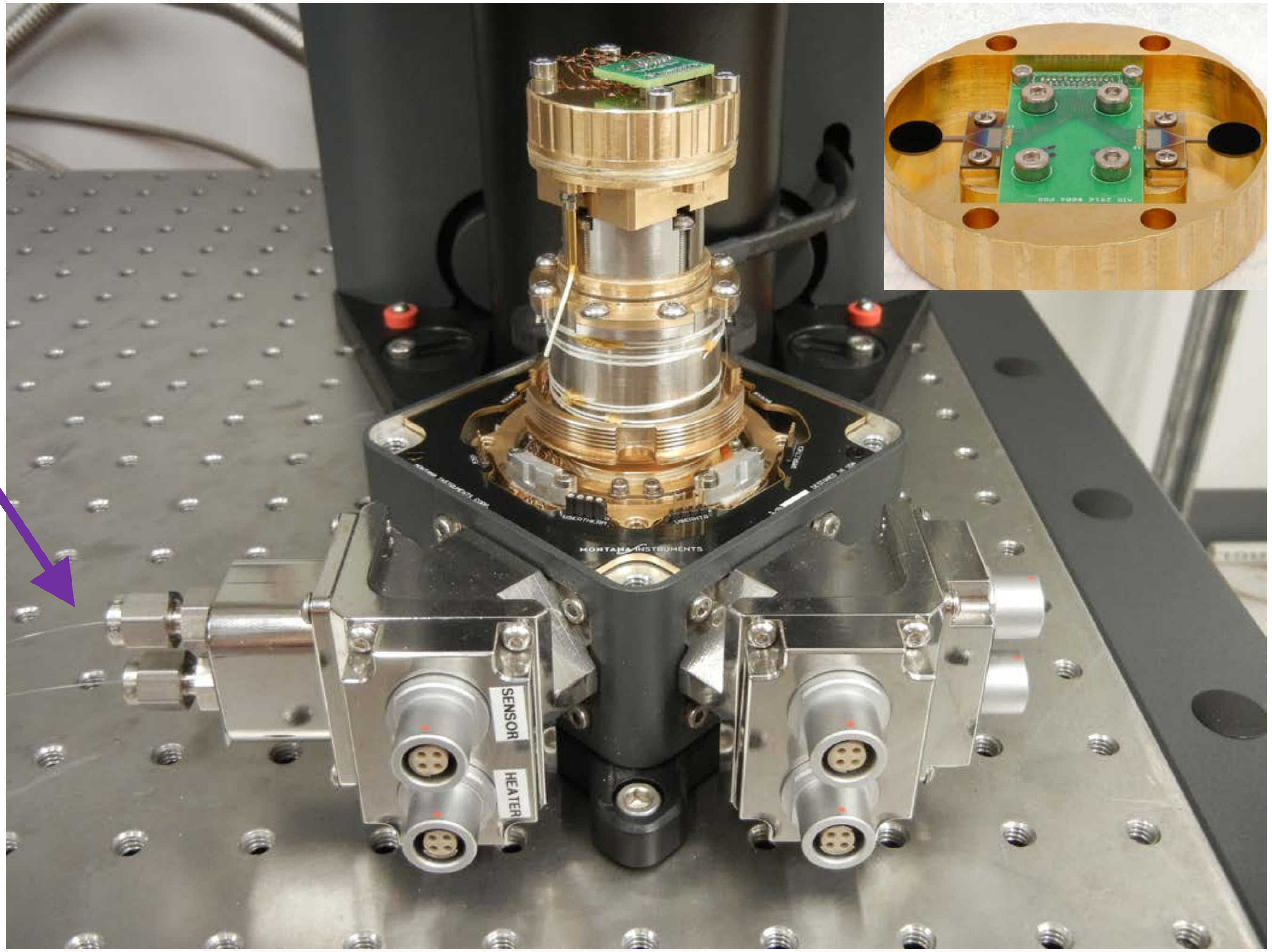

Integration – open beam radiometer (ESR)

- Operation at 200 µW

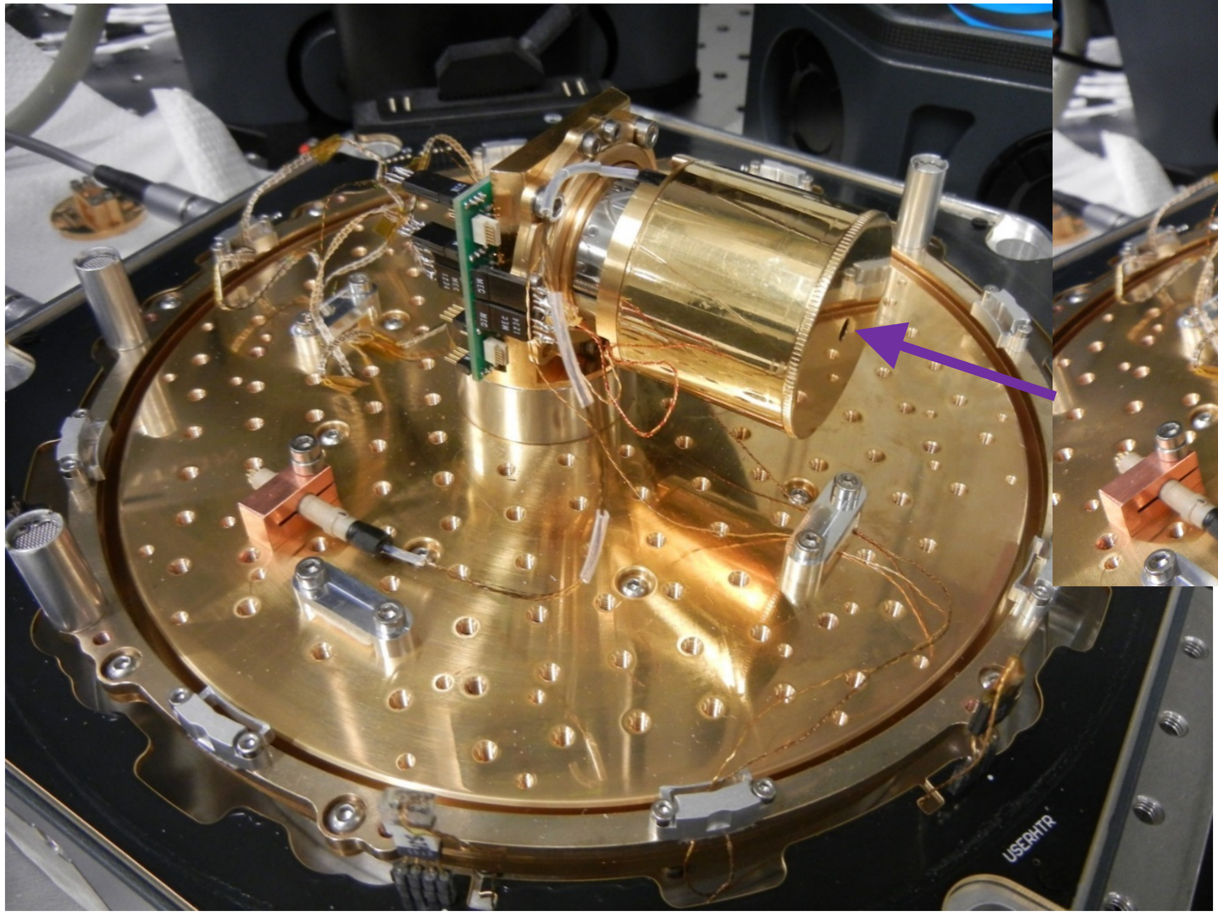

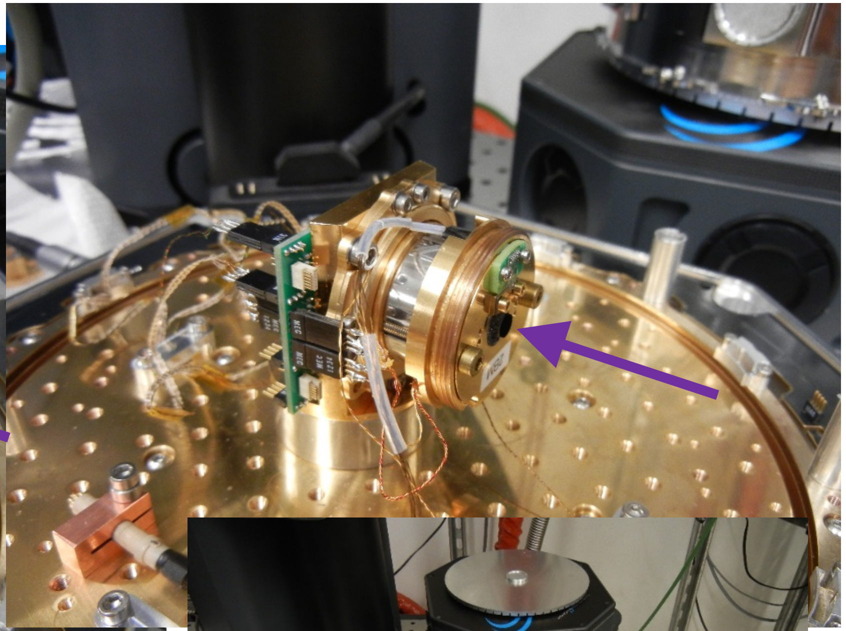

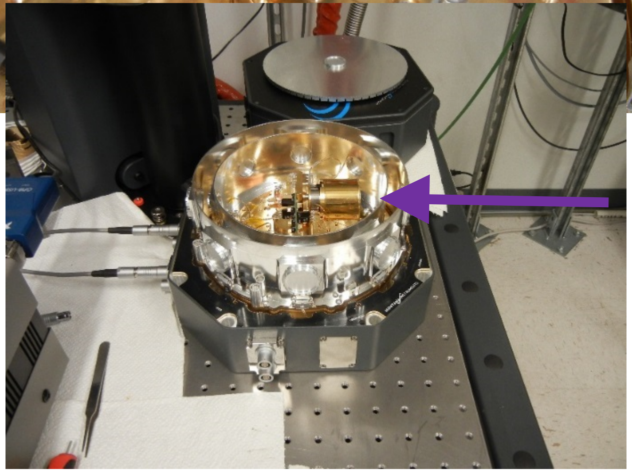

J. Lehman, A Steiger, N.A. Tomlin, M. White, M. Kehrt, I. Ryger, M. Stephens, C. Monte, I. Mueller, J. Hollandt, M. Dowell Optics Express, ***24,*** *23 (2016) https://doi.org/10.1364/OE.24.025911*

Physical Measurement Laboratory

Integration – RC filters & thermal stability

Example: the 3 dB cutoff frequency f_c for a filter with an *RC* of 180s is 0.88 mHz. This attenuates the 1.4 Hz temp. fluctuation of the cryocooler by 1000 x or 30 dB.

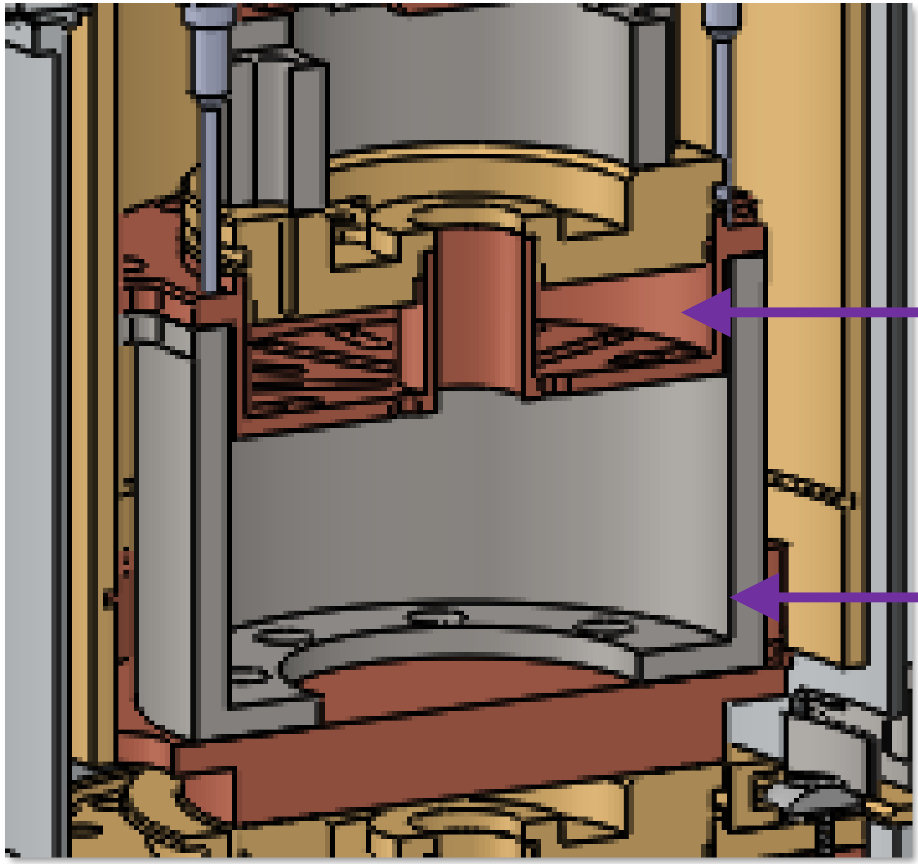

Thermal Capacitor C_p *(J / K)*

Thermal Impedance *R (K / W)*

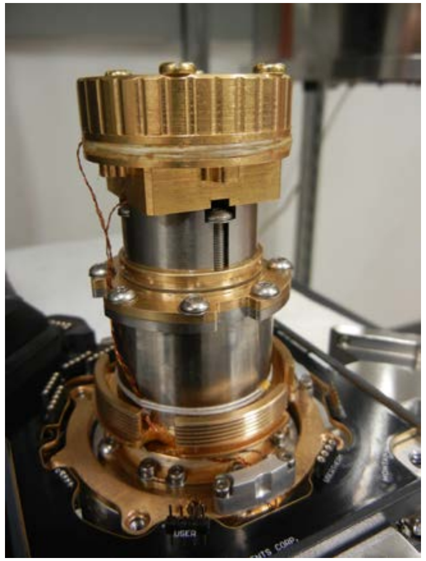

$$f_c = \frac{1}{2\pi RC} = 0.884 \text{ mHz} \Rightarrow 10 \times \log \frac{1.4 \text{ Hz}}{8.84 \times 10^{-4}} = 32 \text{ dB}$$

Integration – damper materials

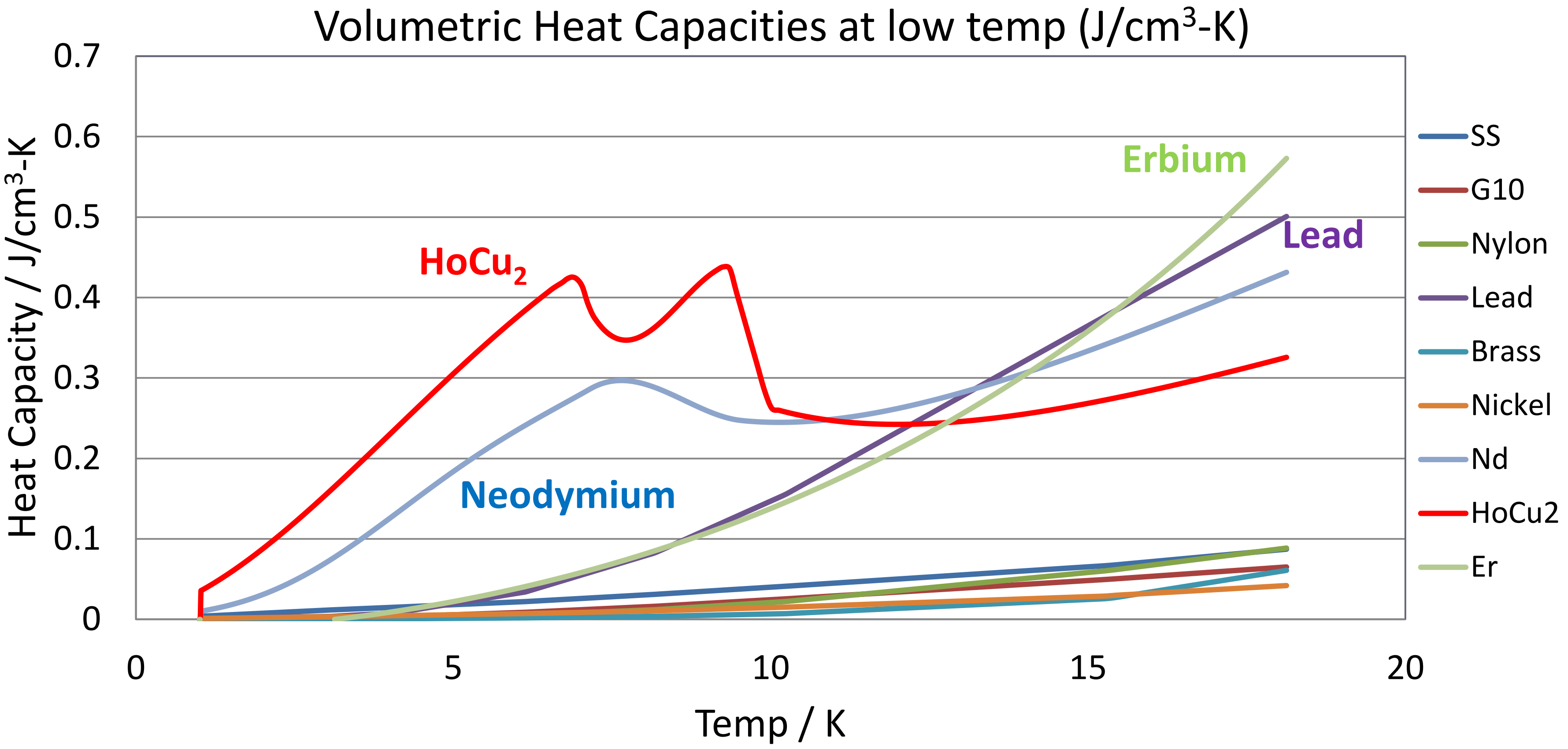

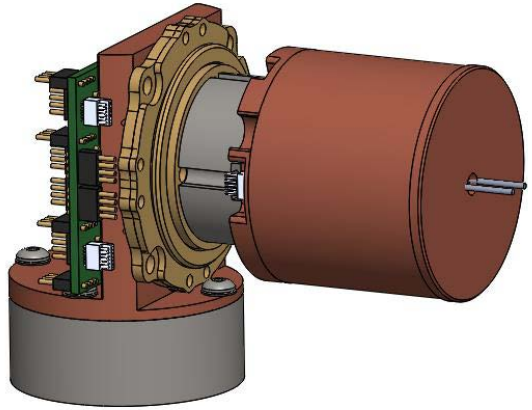

Stainless Steel Damper

For a periodic time dependent thermal fluctuation $\Delta T(x) = \Delta T(0)\exp(-x/\delta_{th})$, where x = distance, δ_{th} the thermal penetration depth; that depth at which the amplitude has dropped to 1/*e* of its initial value, defined as:

$\boldsymbol{\delta_{th}} = \sqrt{\frac{\boldsymbol{\alpha}}{\boldsymbol{\pi f}}}$ α = thermal diffusivity of the material and *f* the frequency of the driven temp. oscillation.

Integration – RC filters

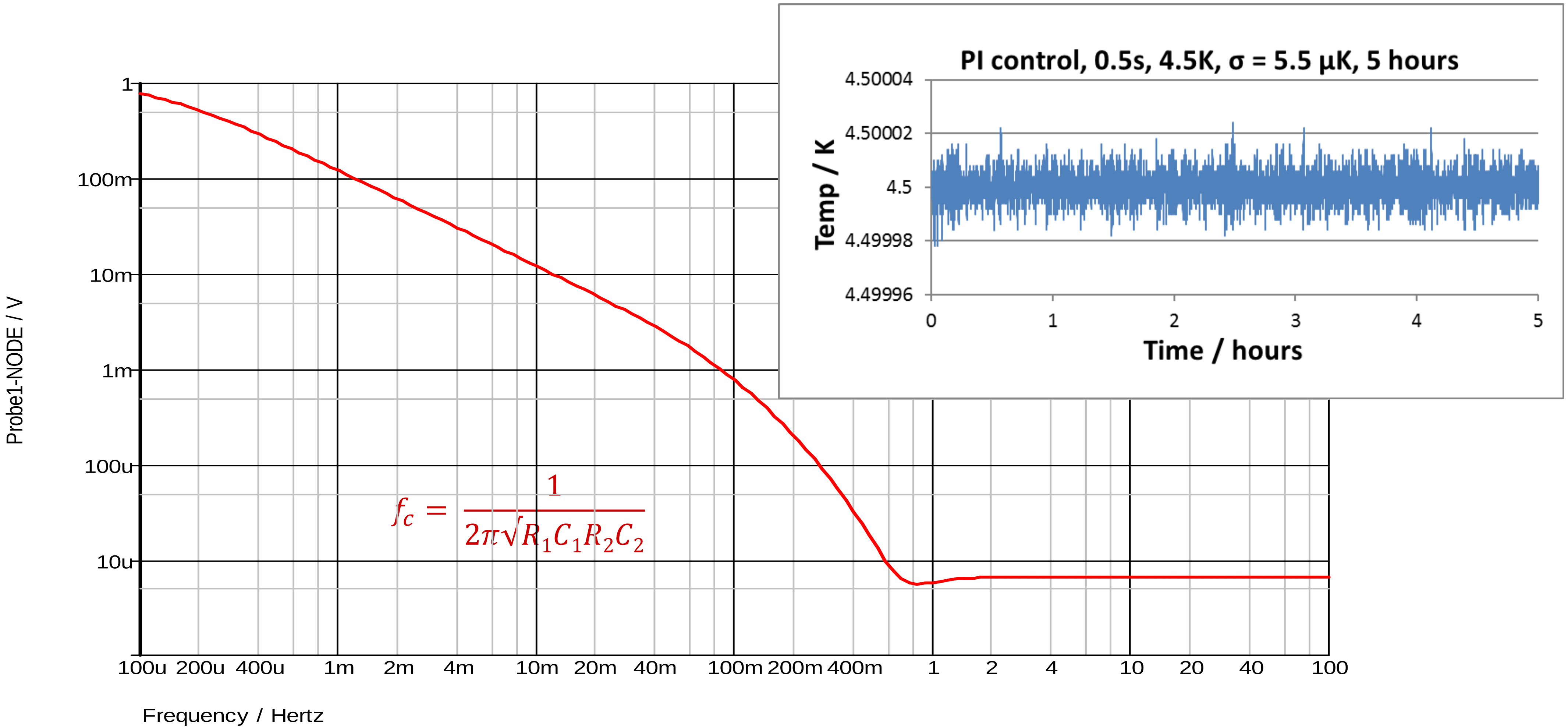

$$f_c = \frac{1}{2\pi\sqrt{R_1 C_1 R_2 C_2}}$$

Thermal stability achieved with 2 pole Butterworth filter, 20 dB / decade - optimised design

Integration – effectiveness of filtering

- Temperature and Resistance noise spectrum of thermal system
- Commercial AC resistance bridge, sampled at 5Hz, 10 mV excitation, constant current

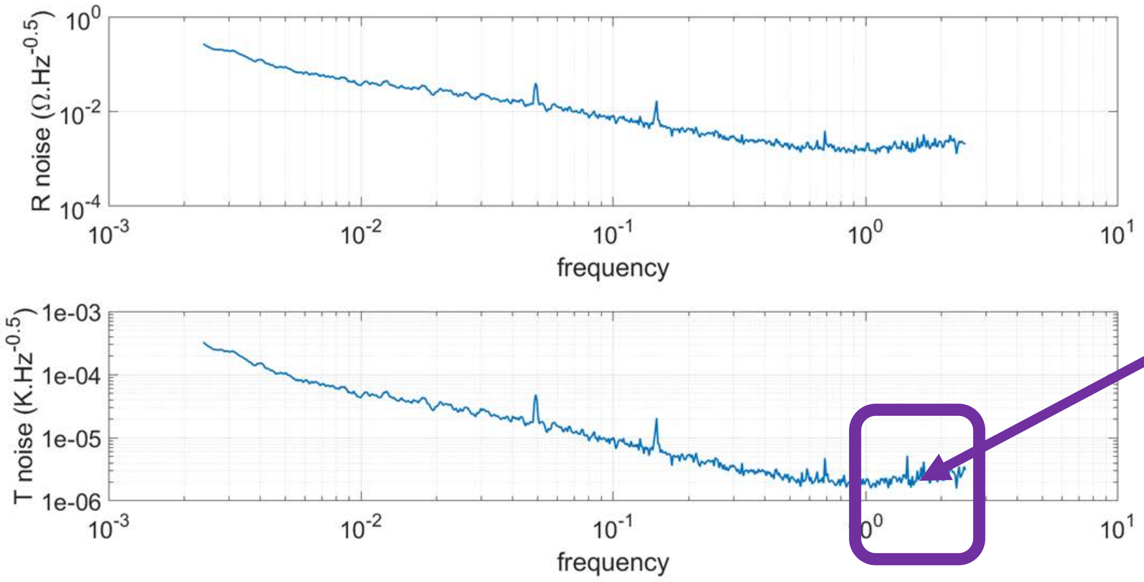

No excitation at 1.4 Hz

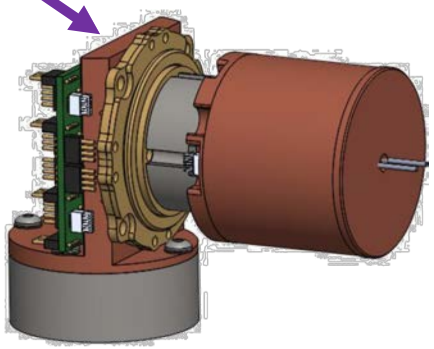

Effectively 50 dB of attenuation of the 1.4 Hz signal; from 200 mK pk-pk to 2 uK (5 µK)

Integration – thermal profile @ 1 mW

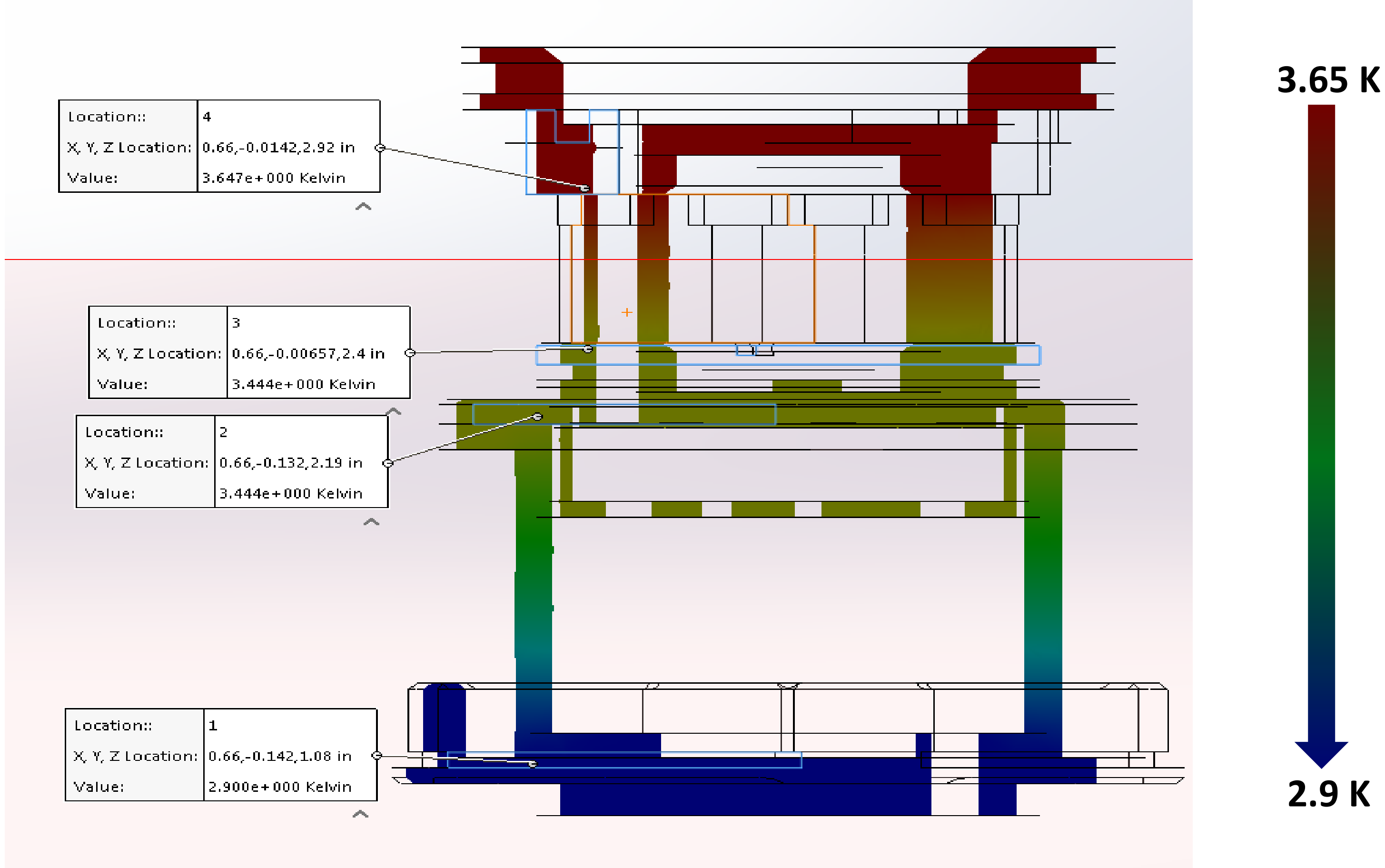

1 mW input power: 0.55 K temp rise across 1st stage RC filter, 0.2 K across 2nd stage

Results – uncertainties

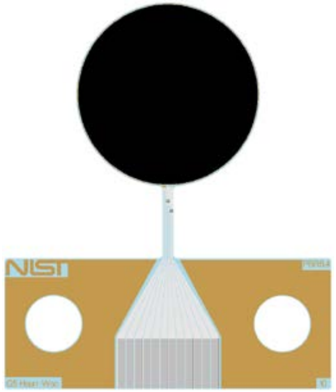

=

?

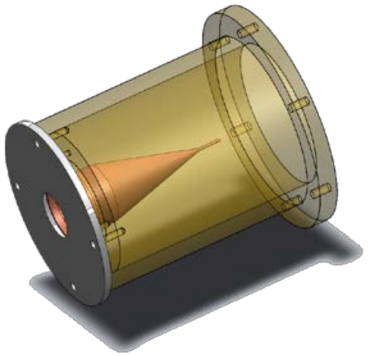

Results – offset

open beam system

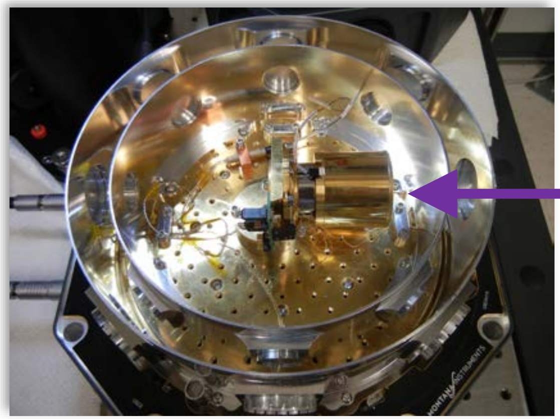

beam

- 0.1 % offset in power

dual fibre system

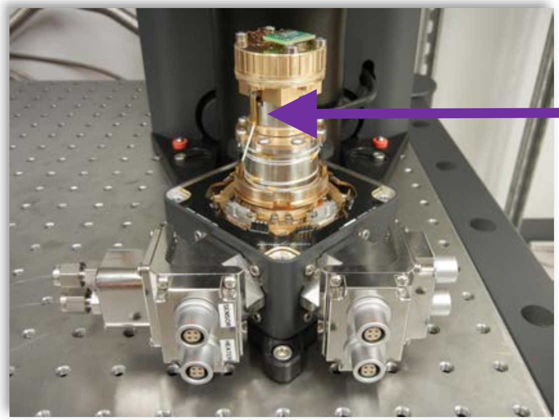

fibre

+ 0.4 % offset in power

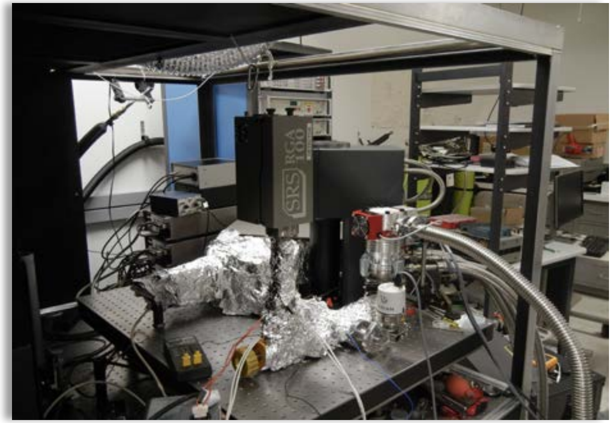

- Reflectance measured at room temp but used at 4 K. Morphological change? Have seen R increase by 10 %
- FC / APC fibre – tip heating up at 4 K and being absorbed by chip detector
- Refractive index of fibre changes at 4 K - typically 0.2 % increase

Results – actual setup

- Chip detectors' reflectance measured at *LASP*
- Offset measured in cryogenic radiometer, detector mounted in fibre system
- Beam-splitter ratio determined

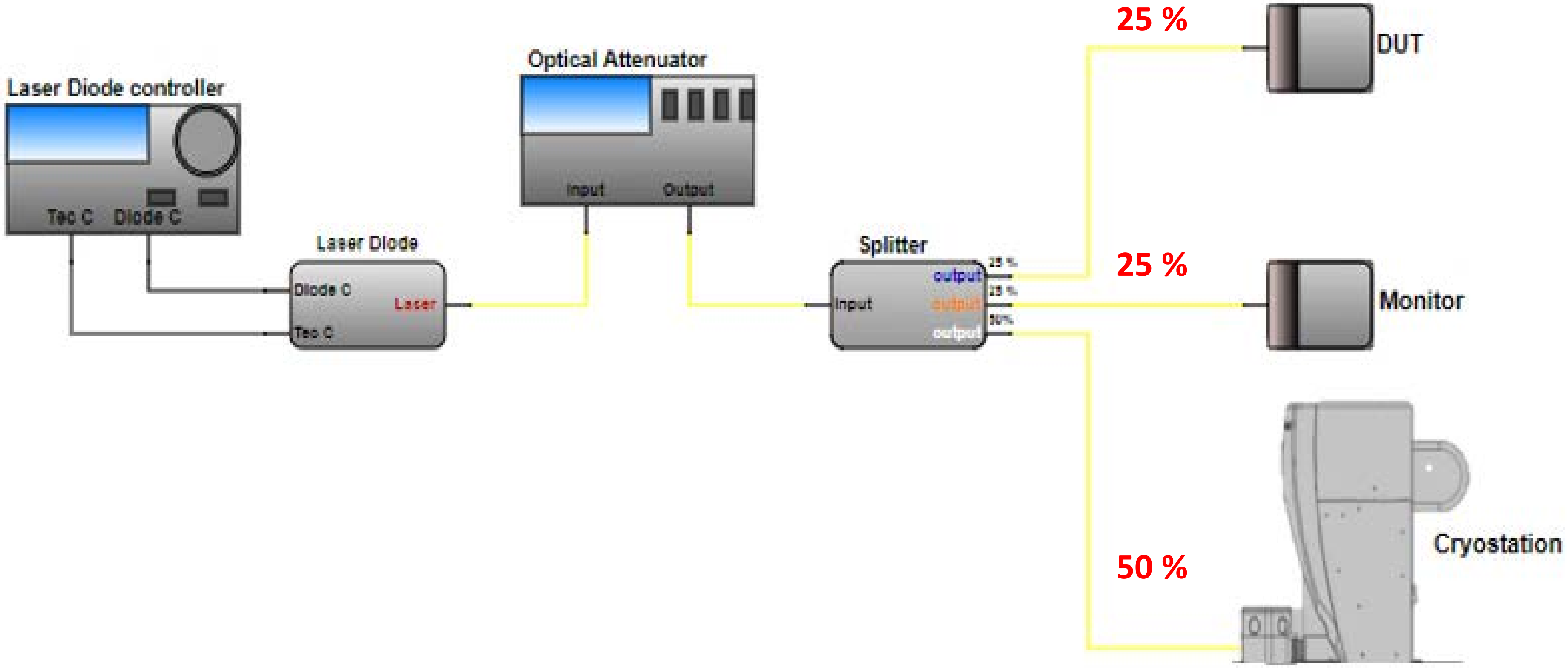

Physical Measurement Laboratory

Results – actual setup

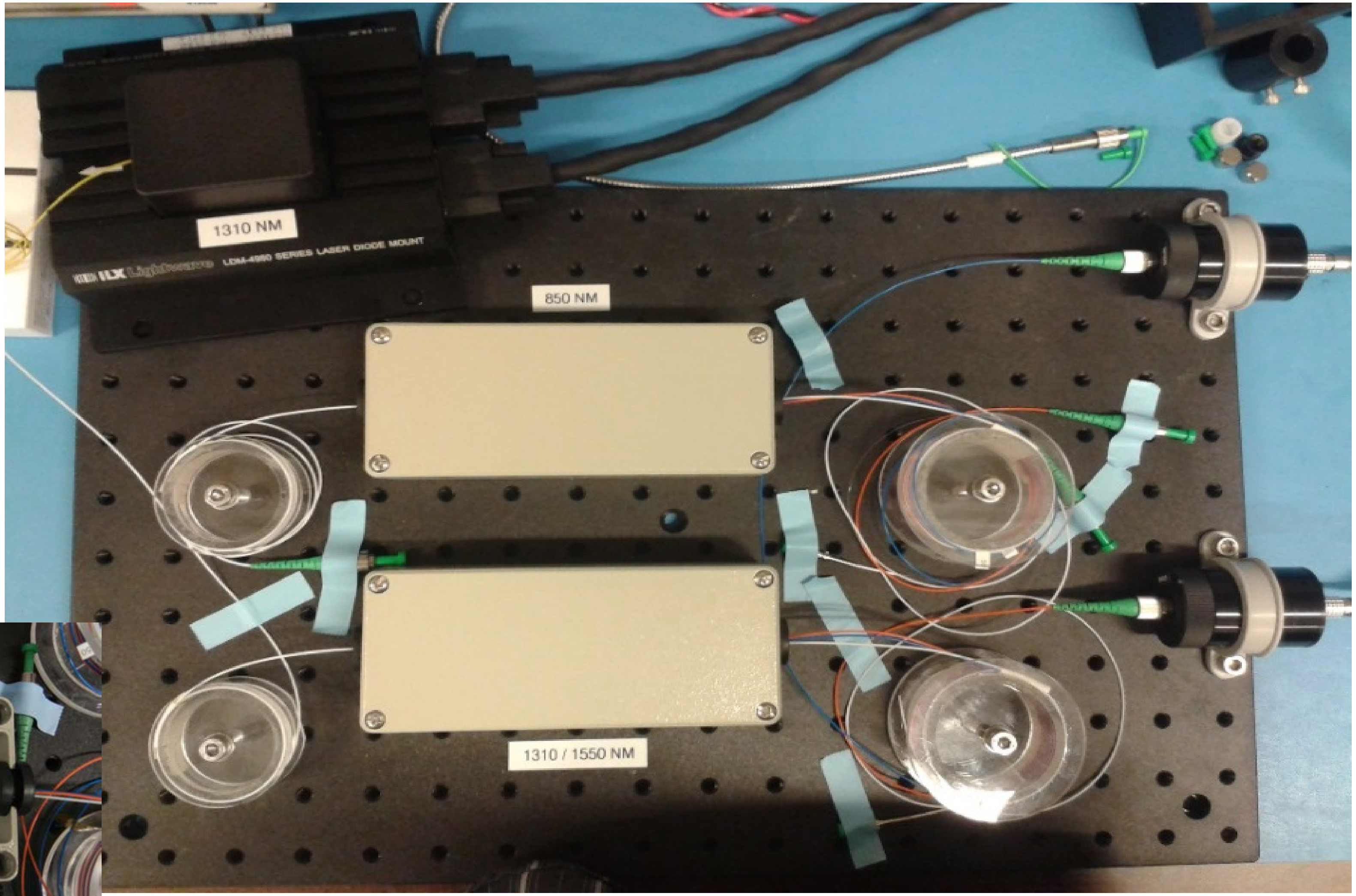

beamsplitter

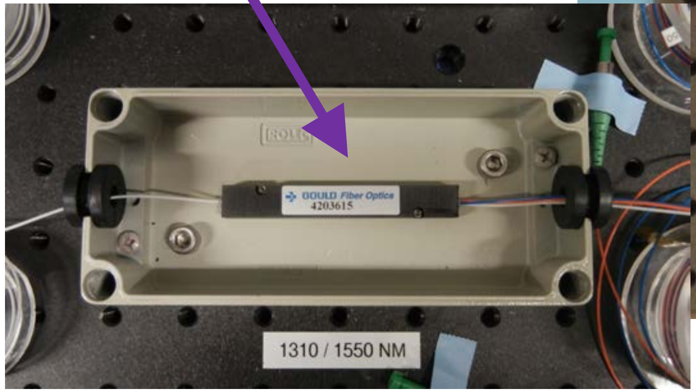

Results – beamsplitter ratio @ 1310 nm

Std dev < 0.01 % over 12 hours, monitoring output with InGaAs detectors, airside

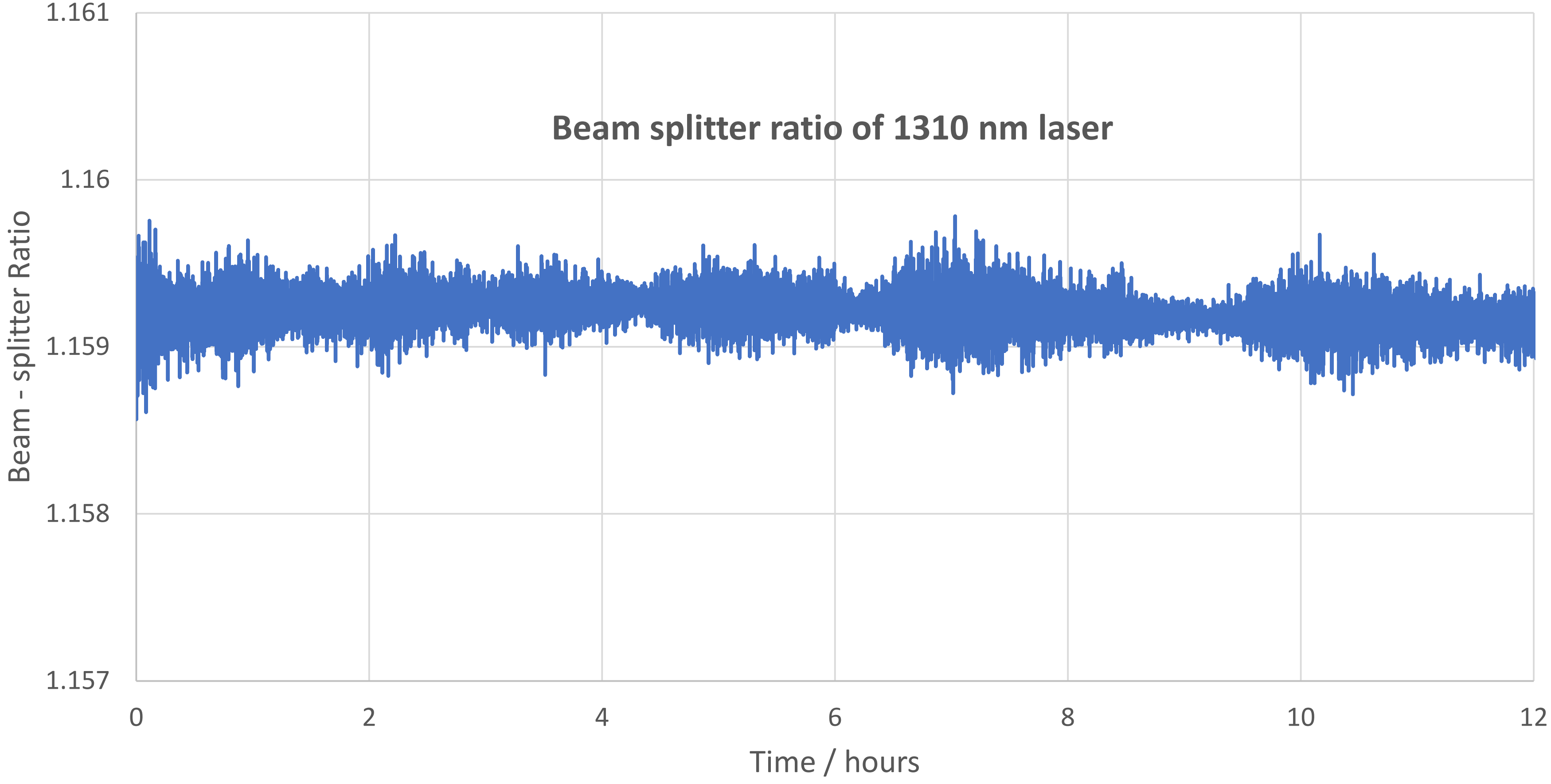

Results – CNT detector offset uncertainty

Uncertainty components of CNT chip detector offset compared to a trap detector @ 633 nm

Component of Uncertainty	[1]δ_i (%)	Distribution	Type	Std Unc (%)
CNT detector absorptance	0.0100	rectangular	B	0.0060
Brewster window transmittance	0.0012	rectangular	B	0.0007
Alignment	0.0017	rectangular	B	0.0010
Heating inequivalence	0.0050	rectangular	B	0.0030
Trap traceability to primary standard	0.0200	normal	B	0.0100
Beam scatter losses	0.0040	rectangular	B	0.0025
NIST electrical power measurement	0.0005	rectangular	B	0.0003
Repeatability of measurement (N = 9)[2]	0.0100	normal	A	0.0033
Combined Standard Uncertainty:				**0.012 %**
Expanded Uncertainty (*k* = 2):				**0.025 %**

[1]$\pm\delta_i$ represents the limits of the estimated uncertainty of the measurand

[2]Standard uncertainty expressed as $\delta_i / \sqrt{N}$ = standard error of the mean (SEOM)

Results – beamsplitter uncertainty

Measurement uncertainties in determining the absolute beam-splitter ratio

Component of Uncertainty	[1]δ_i (%)	Distribution	Type	Std Unc (%)
Chip detector offset	0.025	normal	B	0.012
NIST electrical power measurement	0.0005	rectangular	B	0.0003
Beamsplitter polarisation dependence	0.100	rectangular	B	0.058
Beamsplitter ratio stability	0.015	rectangular	B	0.010
Lab std spectral resp. 1310 & 1550 nm	0.020	rectangular	B	0.012
Laser spectral bandwidth	0.020	rectangular	B	0.012
Detector calibration[2]	0.380	rectangular	B	0.220
Repeatability (N = 9)[3]	0.050	normal	A	0.017
Combined Standard Uncertainty:				**0.23 %**
Expanded Uncertainty (*k* = 2):				**0.46 %**

[1]$\pm\delta_i$ represents the limits of the estimated uncertainty of the measurand
[2]Detector calibration could be improved to 0.05 % by direct cal. against cryogenic radiometer
[3]Standard uncertainty expressed as $\delta_i / \sqrt{N}$ = standard error of the mean (SEOM)

Highlights & the future

- ❖ Demonstration of a planar detector that is efficient, fast, and versatile with specs at least equal to that of cavity detectors
- ❖ Establishment of a new family of laser power standards at NIST using planar detectors
- ❖ Capability to be further developed into linear and two dimensional arrays for spectral and imaging applications

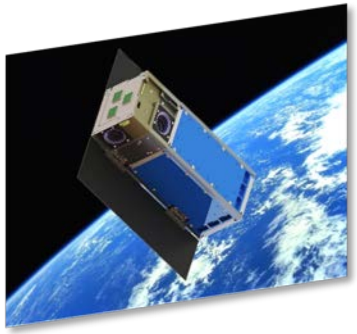

Photo courtesy Blue Canyon Technologies, Boulder

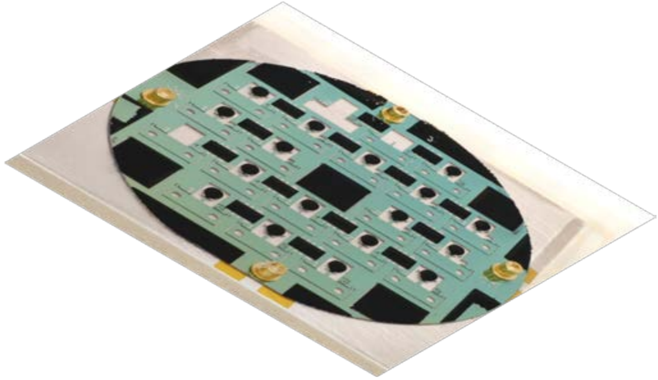

Photo courtesy Nathan Tomlin, NIST

Physical Measurement Laboratory

THANK YOU